

Mechanism of eccrine sweat pore plugging by aluminium salts using microfluidics combined with Small Angle X-ray Scattering

Alice Bretagne, Franck Cotot, Mireille Arnaud-Roux, Michael Sztucki, Bernard Cabane and Jean-Baptiste Galey

Supplementary Information

1) Effect of BSA on ACH-induced plugging of microfluidic channels flowed with artificial sweat.

Figure SI-1 illustrates the key role of proteins in plug formation. Artificial sweat solution without BSA did not produce any insoluble aggregates or plugs. Note that the right hand panels of Fig. SI-1 and Fig. 3 show plugs that are similar in their overall shape, thickness and optical density.

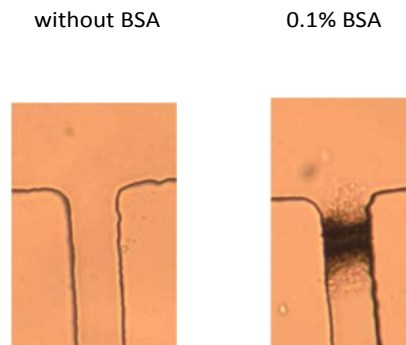


Figure SI-1: Aggregation plugs or absence of plug observed after 15 min with channels flowed by 0.1 nL.s^{-1} artificial sweat with or without BSA and 1 nL.s^{-1} aqueous 15% ACH in surface channel, corresponding to average linear velocities of 36 and $45 \mu\text{m.s}^{-1}$, respectively (sweat channel width = $50 \mu\text{m}$). Artificial sweat used contained 0.5% (w/w) NaCl, 0.1% lactic acid, 0.1% urea at pH 6.5 (adjusted with ammonia) with or without 0.1% BSA

2) Additional SAXS data

Figures SI-2 and SI-3 present a quantitative determination of the concentrations of BSA in each matrix element of the T junction cell described in Figure 6. This information is provided by the calculation of the integral of the scattering, which yields the total fluctuation of electronic density in the irradiated volume. Thus, for each matrix element in the cell near the junction, and at every time, we determined a rescaling coefficient as the ratio of the measured integral to the integral measured in a matrix element of the sweat channel far from the junction, in a place where the channel contained only the pure BSA solution. The expression of the integral of the intensity over all scattering vectors, also called the invariant, is :

$$Q = \int_0^\infty I_{\text{abs}}(q) q^2 dq = 2\pi^2 \langle \eta^2 \rangle /6$$

where $I_{\text{abs}}(q)$ is the absolute scattered intensity per unit volume, equal to the experimental intensity divided by the sample thickness, and $\langle \eta^2 \rangle$ is the average fluctuation of the density of scattering length within the irradiated volume¹.

At early times (6 min), the matrix elements E10 to E7 are well matched by the scattered intensity of BSA and their relative concentrations are 1.04, 1.12, 1.25 and 2.5 times that of the BSA solution. Accordingly, the concentration of aggregates that have accumulated in matrix element is respectively 0.04, 0.12, 0.25 and 1.5 times that of the BSA solution (Table SI-1). The spectra from matrix elements E6 to E3 cannot be matched by the spectrum of BSA, because they contain essentially the scattered intensity from the ACH polycations.

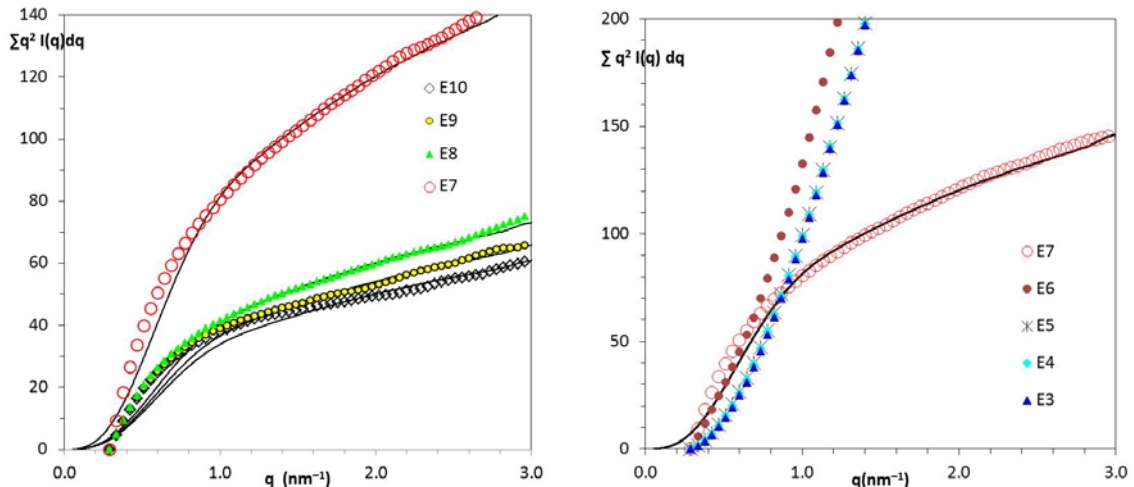


Figure SI-2: Calculation of the concentration of solutes in each cell at short time $t = 6$ min. For each scattering image, the symbols are the data and the full line is the spectrum of the BSA solution scaled to match that of each cell. Vertical: values of the integral of the scattering over all directions of reciprocal space, $\sum q^2 I(q) dq$ (arbitrary units). The high- q limit of this integral is proportional to the average concentration of the solute molecules¹. Horizontal: values of scattering vector q .

At late times (Fig. SI-3), the cells E10 to E6 are well matched by that of BSA and their relative concentrations are 2.9, 3.5, 3.8, 4.8 and 29 times that of the BSA solution (Table SI-1). Accordingly, the concentration of aggregates that have accumulated in each cell is respectively 1.9, 2.5, 2.75, 3.8 and 28 times that of the BSA solution. The spectra from cells E5 to E3 cannot be matched by that of BSA, because they contain mostly the scattering from the ACH polycations.

¹ A. Guinier and G. Fournet, Small Angle Scattering of X-rays, Wiley 1955; O. Glatter and O. Kratky, Small Angle X-ray Scattering, Academic Press 1982; P. Lindner and Th. Zemb, Neutron, X-rays and Light: Scattering Methods Applied to Soft Condensed Matter, North Holland 1982

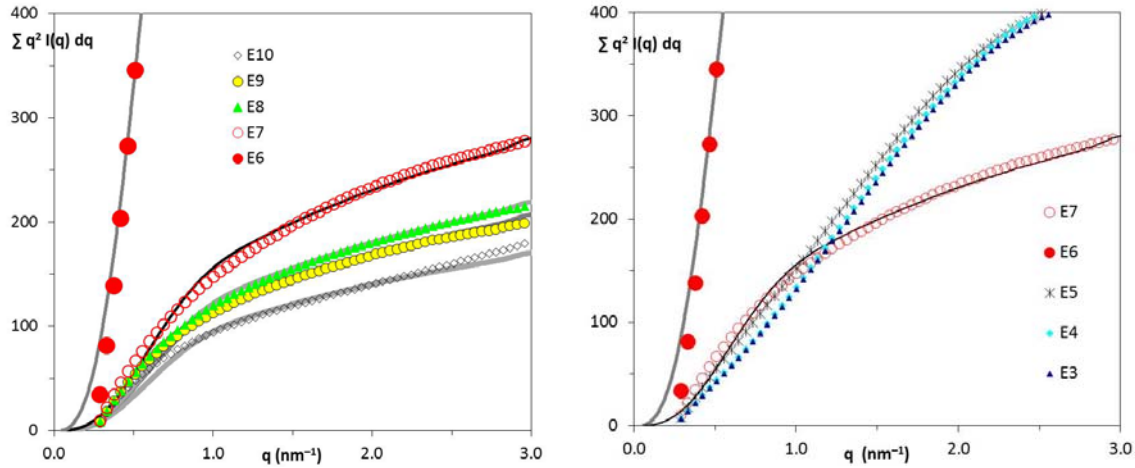


Figure SI-3: Calculation of the concentration of solutes in each cell at long time $t = 32$ min. For each scattering image, the symbols are the data and the full line is the spectrum of the BSA solution scaled to match that of each cell. Vertical: values of the integral of the scattering over all directions of reciprocal space, $\sum q^2 I(q) dq$ (arbitrary units). The high- q limit of this integral is proportional to the average concentration of the solute molecules¹. Horizontal: values of scattering vector q .

Cell number	Scaling factor at 6 min	Scaling factor at 32 min
E10	0.04	1.9
E9	0.12	2.5
E8	0.25	2.8
E7	1.5	3.8
E6	-	28

Table SI-1: values of the scaling factors obtained by matching integral of the scattering with that of BSA.

We explored these phenomena further by measuring the intensity along a horizontal line (6th line from top). These measurements are presented in Fig. SI-4. They show the transfer of « lumps » of scattering material along the line, first to the front of the line ($t = 18$ to 20 min), then to the rear ($t = 22$ to 24 min), then back to the center ($t = 26$ - 32 min). These displacements of large amount of connected material across the junction appear to precede the onset of faster accumulation kinetics (see the increase in accumulation rate that takes place after the displacement at $t = 20$ - 24 min). We interpret these phenomena by assuming that hydrodynamic forces push small pieces of gel into locations where they effectively plug the flow and lead to a faster accumulation of proteins into the plug.

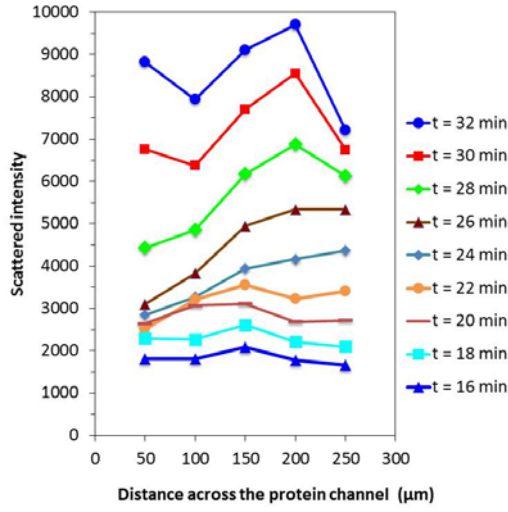


Figure SI-4: Profiles of intensity scattered at low q values by cells located along a horizontal line (6th line from top).

Figure SI-5 shows the impact of structural parameters on scattering intensity fit, in complement to Figure 5 (scattering intensities from the separated components of the system). In order to give an idea of the precision in the determination of the mass per polycation, we have changed the fit parameters for the ACH spectrum showing spectra for 19, 25 or 33 Al atoms.

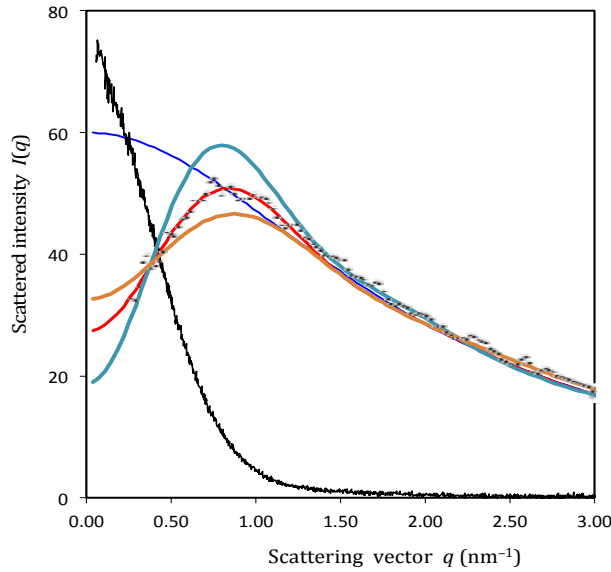


Figure SI-5: SAXS spectra from both solutes ACH and BSA, each one alone in water. Full black line: spectrum from a 1% BSA solution. Black dots: spectrum from a 1% ACH solution. Blue line: model for repelling branched ACH polymers containing 33 Al atoms. Full red line (same as in Fig. 5): model for 25 Al atoms. Orange line: model for 19 Al atoms. Structural parameters used to fit the scattering intensity plot: volume fraction ACH = 0.068, fractal dimension ACH = 2.1, gyration radius ACH = 0.9 nm, repulsion length = 5.5 nm, ACH scale factor = 60.

Figure SI-6 presents the scattered intensity measured along the central column at long times, shortly after plug expulsion. The SAXS spectra can then be decomposed into a contribution from free proteins and another one from free polycations. The fits are the interdiffusion profiles of polycations into the protein solution and of proteins into the polycation solution, calculated from Fick's law for one-dimensional diffusion of a solute from a fixed boundary.

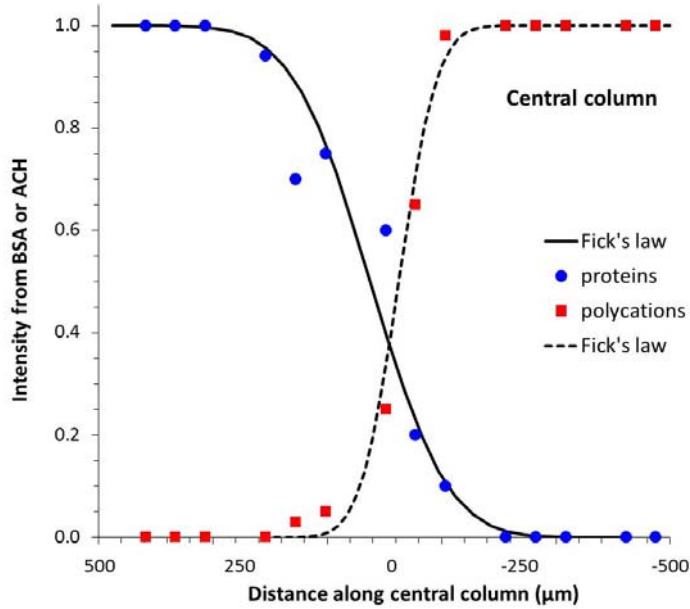


Figure SI-6: Relative intensities scattered at very long times by cells along the central column. The intensity scattered by each cell can be decomposed into a contribution from BSA (dark blue dots) and a contribution from free ACH (red dots).



a) Supplementary **Movie M1** associated to **Fig. 3**.

Typical aggregation patterns observed with microfluidic chip flowed by 0.1 nL.s^{-1} natural eccrine sweat and 1 nL.s^{-1} aqueous 15% ACH in surface channel, corresponding to Figure 3 conditions (sweat channel width = $50 \mu\text{m}$). Video rate: one image every minute.

b) Supplementary **Movie M2** associated to **Fig. 4**.

Typical aggregation patterns observed with V2 microfluidic chip flowed by 0.5 nL.s^{-1} artificial sweat containing 0.1% BSA ($15 \mu\text{M}$) and 1 nL.s^{-1} aqueous 15% ACH in “surface channel”, corresponding to Figure 4 conditions (channel width $300 \mu\text{m}$). Video rate: one image every 15 s.